PHYSICAL REVIEW B VOLUME 17, NUMBER 8 15 APRIL 1978

# Approach to the embedding problem in chemisorption in a self-consistent-field–molecular-orbital formalism

C. Pisani
*Institute of Theoretical Chemistry, University of Turin, Via P. Giuria 5, I-10125 Torino, Italy*
(Received 5 October 1977)

A solution for the embedding problem in chemisorption is proposed, particularly designed for easy implementation into molecular-orbital linear-combination-of-atomic-orbitals self-consistent-field calculation schemes. It is essentially based on the assumption that the perturbation in the electronic states induced by the adspecies is effectively screened within a certain $B$ region of the adsorbing solid and that this $B$ region is also large enough to allow for neglect of direct-coupling terms between the adspecies and the defective solid. An energy-dependent coupling matrix $M(e)$ is defined, which may be calculated on the basis of the free-solid solution and that can be used to correct the local solutions so as to properly connect them to the free-solid ones. The theory is tested in the case of hydrogen adsorption on graphite in the complete neglect of differential overlap approximation. Moderately large embedded clusters appear to be adequate for a correct description of the chemisorption process.

## I. INTRODUCTION

A number of recent papers (see for instance Refs. 1–6 and references therein) report about calculations performed by ordinary quantum-chemistry techniques to study small clusters of atoms from a solid and their interactions with outer atoms or molecules. Such kind of calculations are proving very useful for a preliminary characterization of the chemical behavior of specific surface sites. It is apparent however that such models are a crude approximation to a real surface, the large majority of atoms included in the calculation usually having not even the proper surrounding of nearest neighbors. Boundary effects are therefore important and convergence with respect to increasing cluster size is expected to be slow.[7] On the other hand, self-consistent calculations of the electronic structure of solids with a surface, with or without regular chemisorbed phases thereupon, are beginning to be performed.[8–11] In this case, one can take advantage of bidimensional translational symmetry; still, computational problems are formidable.

If one is interested in the electronic response of a solid to a local perturbation at the surface, e.g., due to an absorbed species, it would therefore be desirable to take full profit of such computations by combining a local self-consistent treatment with an embedding scheme insuring the proper connection with the rest of the solid.

The formal theory of embedding was developed and discussed recently by Grimley[12–14] and an approximate solution scheme has been proposed and tested relying on Green's-function techniques.[7,14] An important step towards the feasibility of realistic chemisorption calculations using properly embedded clusters was made by Gunnarsson and Hjelmberg.[15,16] They generalized Grimley's method and introduced well-motivated approximations essentially amounting to assume that the perturbation induced by the adatom is confined within a limited region, where the solution is developed into a finite set of localized functions. Their method was developed and implemented within the framework of Kohn and Sham[17] theory with the local spin-density approximation for exchange and correlation, and is probably best suited for studying adsorption on nearly-free-electron-like metals.

If local potentials or pseudopotentials are considered, methods as proposed by Appelbaum and Hamann for the study of surfaces[8] can be used: in the perturbed region, a self-consistent solution is numerically found, which is smoothly joined to the solution appropriate for the infinite unperturbed substrate. However, such a method is not easily applicable to chemisorption problems and is not compatible with standard quantum chemistry programs.

An example of a possible different kind of solution to the embedding problem is provided by the work of Doyen and Ertl[18,19]; in that case, a transformation of the metal eigenfunction is performed such as to effectively reduce the chemisorption problem to a surface molecule one; however, their method is specific of the Hamiltonian they have introduced.

In the present paper, a new scheme for the study of chemisorption on embedded clusters is worked out, starting from Grimley's formulation and based on approximations similar to those involved in the work of Gunnarsson and Hjelmberg. However, the choice of the approximations and the development of the resulting equations are especially

 

designed as to allow a quite simple implementation of this embedding scheme into molecular-orbital self-consistent-field linear-combination-of-atomic-orbitals (MO-SCF-LCAO) programs based on any local or nonlocal effective one-electron Hamiltonian.

Besides that, the method presents two attractive features: first, it is exact in both limits of large clusters size, and, for arbitrary cluster size, of negligible interaction with the adspecies; second, the key quantity used for performing the embedding is an energy dependent coupling matrix $M(e)$ which only depends on the characteristics of the adsorbing substrate, and therefore may be calculated once for all when the solution for the free substrate is known.

In Sec. II the theory is presented and the approximations discussed; in particular it is shown that the cluster must be large enough to make it reasonable to assume that direct coupling terms between the adspecies and the defective solid are effectively screened. A workable scheme for actual computations is also introduced.

In Sec. III a number of preliminary calculations are reported intended to demonstrate the feasibility of the method and to assess its limits of applicability. They concern the adsorption of a hydrogen atom on a graphite monolayer using a Hartree-Fock (HF) Hamiltonian in the complete neglect of differential overlap (CNDO) approximation. Although the CNDO scheme is still widely used for studying different kinds of solids and adsorption thereon,[5,20,21] the main reason for adopting it here (and indeed for considering the hydrogen-graphite system) was that we disposed of a very accurate solution for the graphite monolayer and had studied its interaction with hydrogen adlayers in that approximation.[11,22] It may also be argued that, among semiempirical methods, the CNDO approach bears strongest formal resemblance to sophisticated *ab initio* methods, so providing a good and economical test ground for hypotheses. The results obtained and possible future developments are finally discussed.

## II. METHOD

### A. Embedding equations

The system to be studied is represented schematically in Fig. 1. Assume that a set of localized functions $\{\chi_\mu\}$ is available, centered on the adsorbate ($A$), on that ($B$) part of the solid which belongs to the adsorption cluster, and on the "defective solid" $D$. For definiteness, take these functions to consist of a small number of atomic orbitals per each atom; overcompleteness problems[13,15] are unimportant for this basis set.

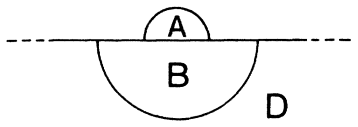


FIG. 1. Scheme for the partition of the basis set. The cluster $(A \cup B)$ will be denoted by $C$ in the text, and the solid $(B \cup D)$ by $S$.

Consider now any one-electron Hamiltonian $\hat{F}$ (for instance the HF or an effective Hamiltonian derived according to Kohn-Sham theory) and its representation $F$ in the given basis. Its matrix elements will generally be dependent on the density matrix $P = \{\langle a_\mu^\dagger a_\nu \rangle_0\}$; a self-consistency problem arises which, for subsequent reference, is most conveniently expressed in the formalism of Green's functions[13]

$$\begin{aligned} &Q(\zeta)G(\zeta) = I\,, \\ &Q(\zeta) = \zeta S - F[P], \quad \zeta = \epsilon + i0\,, \\ &P = -\frac{2}{\pi}\,\mathrm{Im}\int_{-\infty}^{\epsilon_F} d\epsilon\, G(\zeta)\,, \end{aligned} \tag{1}$$

where $S$ is the overlap matrix and the Fermi level $\epsilon_F$ is determined by the number of electrons in the system. Of course, the system (1) is the exact counterpart of the more familiar system of equations

$$\begin{aligned} &FA = SAE, \quad E_{ij} = e_i \delta_{ij}\,, \\ &P = A^* O \tilde{A}, \quad O_{ij} = 2\delta_{ij}\Theta(\epsilon_F - e_i)\,, \\ &A^\dagger S A = I\,. \end{aligned} \tag{2}$$

The equivalence of (1) and (2) will be exploited in the following. Note that for simplicity of notation the whole treatment is developed for a closed shell configuration, its generalization to different orbital for different spin (DODS) cases being straightforward.

Using the partition schematically illustrated in Fig. 1, Eq. (1) may be developed exactly in the cluster $C$ region as follows:

$$\begin{aligned} &Q_{AA}G_{AA} + Q_{AB}G_{BA} + Q_{AD}G_{DA} = I^A\,, \\ &Q_{AA}G_{AB} + Q_{AB}G_{BB} + Q_{AD}G_{DB} = 0\,, \\ &Q_{BA}G_{AA} + Q_{BB}G_{BA} + Q_{BD}G_{DA} = 0\,, \\ &Q_{BA}G_{AB} + Q_{BB}G_{BB} + Q_{BD}G_{DB} = I^B\,. \end{aligned} \tag{3}$$

The local character of the perturbation induced by the adsorbed species and the "large size" of the $B$ region will now be taken into account by adopting the following approximations: (a) Matrix elements of $Q$ and $G$ involving basis functions which belong

to the defective solid, are frozen at their "free solid" value (hereafter specified by an $f$ superscript): $Q_{BD}=Q^f_{BD}$, $G_{DD}=G^f_{DD}$, etc. (b) Compound quantities such as $Q_{AD}G_{DB}$ or $Q_{AB}G_{BD}$, involving $A$-type and $D$-type functions, are negligible with respect to unity. (c) Finally, due to the vanishingly small ratio of the number of electrons provided by the adspecies with respect to the number of electrons in the adsorbent, the Fermi level is assumed to stay fixed at the value appropriate for the free solid: $\epsilon_F=\epsilon^f_F$. In a nonconducting solid this is made to correspond to the bottom of the conduction band.

The above approximations essentially amount to admit that the effect of $A$ is adequately screened within $B$, at least if one is not interested in subtle phenomena (for instance, long-range interference between adatoms). In metals, screening of local perturbations by conduction electrons appears to be very effective and Friedel charge oscillations are rapidly quenched; this may be a reason why, in these cases, local schemes meet with unexpected success.[23] Long-range influence of local perturbations are of course likely to occur in insulators and semiconductors, but it is possible that space-charge effects could be taken into account of in a semiclassical way[24] after performing the computation.

Approximation (a) and assumption (c) are adopted in Gunnarsson and Hjelmberg theory.[15] These authors do not introduce formally approximation (b), but some of its implications are contained in the approximating simplifications leading to their final formula.

In approximation (b) the decoupling effect of the $B$ region enters more clearly into play. It is not implied that individual $Q_{\mu\nu}(\epsilon)G_{\nu\sigma}(\epsilon)$ products are negligible, although it is certainly true that, with increasing distance between centers, the $G$ matrix and especially the $Q$ matrix elements are decreasing in absolute value (see Sec. III). Rather, the size of $B$ insures that from sums such as $\sum^B_\nu Q_{\mu_A\nu}G_{\nu\sigma_D}$ or $\sum^D_\nu Q_{\mu_A\nu}G_{\nu\sigma_B}$ dominant terms are absent and destructive interference effects are important, since they involve a large number of terms of comparable size and different sign.

At the end, the validity of the proposed scheme must certainly be evaluated by a critical examination of the results it leads to. However, it is evident that all approximations are strictly valid in both limits of very large size of $B$ and of absence (or negligible interaction) of the adparticle; these fundamental characteristics must also be found in the final equations (see Sec. IIB).

Inserting (a) and (b) approximations into Eq. (3), we obtain, after observing that $I^B-Q^f_{BD}G^f_{DB}=Q^f_{BB}G^f_{BB}$,

$$\begin{aligned}
&Q_{AA}G_{AA}+Q_{AB}G_{BA}=I^A\,,\\
&Q_{AA}G_{AB}+Q_{AB}G_{BB}=0\,,\\
&Q_{BA}G_{AA}+Q_{BB}G_{BA}=0\,,\\
&Q_{BA}G_{AB}+Q_{BB}G_{BB}=Q^f_{BB}G^f_{BB}\,,
\end{aligned}\tag{4}$$

or

$$Q^CG^C=J^C\,,\qquad J^C=\begin{bmatrix} I^A & 0\\ 0 & Q^f_{BB}G^f_{BB}\end{bmatrix}.$$

To self-consistently solve the system (4), we introduce an auxiliary $\bar G^C$ matrix, which is just the inverse of $Q^C$, and again use approximation $b$,

$$\begin{cases} Q^C\bar G^C=I^C\,,\\ G^C=\bar G^CJ^C\,,\\ Q^C=\zeta S^C-F^C[P]\,,\\ P^C=-\dfrac{2}{\pi}\,\mathrm{Im}\displaystyle\int_{-\infty}^{\epsilon^f_F}d\epsilon\,G^C(\zeta)\end{cases}$$

$$-\begin{cases} G_{AA}=\bar G_{AA}\,,\\ G_{AB}=\bar G_{AB}-(\bar G_{AB}Q^f_{BD})G^f_{DB}\cong\bar G_{AB}\,,\\ G_{BA}=\bar G_{BA}\,,\\ G_{BB}=\bar G_{BB}Q^f_{BB}G^f_{BB}\,.\end{cases}\tag{5}$$

At each iteration cycle the $P$ dependent $Q^C$ matrix must be redefined. However, since we admit that quantities involving $D$-type functions stay fixed at their free solid values, only those terms which involve $P$ elements within the cluster have to be changed; the self-consistency problem is so really confined to within the cluster. For example, for a HF Hamiltonian we can write

$$\begin{aligned}
&F^C=F^C_0+L^C\,,\\
&L^C=\begin{bmatrix}0^A & 0\\ 0 & L^B\end{bmatrix},\\
&L^B_{\rho\sigma}=F^f_{\rho\sigma}-\Big(\sum_{N\in B}\Big\langle\rho\Big|\frac{Z_N}{|r-r_N|}\Big|\sigma\Big\rangle+\langle\rho|\hat t|\sigma\rangle\\
&\qquad+\sum_{\mu\nu}^{B}P^f_{\mu\nu}[(\rho\sigma|\mu\nu)-\tfrac12(\rho\mu|\sigma\nu)]\Big).
\end{aligned}\tag{6}$$

Here $F^C_0$ designs the HF matrix formally calculated as if the problem were restricted to the cluster, but using the $P^C$ matrix appropriate for the embedded cluster. That is, the correction terms are obtained by subtracting from the free solid Hamiltonian, those terms which are already in-

cluded in $F_0^C$. In the last line (and in the following) $\sum^B$ designates sums which are extended to all basis functions belonging to set $B$.

It is seen that the correction matrix $L^B$ is a constant during iterations and contains only quantities which are available from the free solid calculation ($F^{Bf}, P^{Bf}$) and integrals involving basis functions of set $B$, which are needed also for calculating $F_0^C$.

To calculate $\bar{G}^C$, we take profit of the equivalence of Eqs. 1 and 2, and perform a diagonalization of $F^C[P]$,

$$F^C\bar{A} = S\bar{A}\bar{E}\,,$$
$$\bar{G}_{\mu\nu}(\zeta) = \sum_j \frac{\bar{a}_{\mu j}\bar{a}_{\nu j}}{(\epsilon - \bar{e}_j + i0)} \tag{7}$$

(the basis set of the eigenvectors are assumed to be real). Using the formal identity

$$\bar{G}_{\mu\sigma}(\zeta)Q^f_{\sigma\tau}(\zeta)G^f_{\tau\nu}(\zeta) = \sum_{ij} \frac{\bar{a}_{\mu j}\bar{a}_{\sigma j}[(\epsilon+i0)S_{\sigma\tau} - F^f_{\sigma\tau}]a^f_{\tau i}a^f_{\nu i}}{(\epsilon - \bar{e}_j + i0)(\epsilon - e^f_i + i0)} = \sum_j \left[\mathcal{P}\left(\frac{\bar{a}_{\mu j}\bar{a}_{\sigma j}}{\epsilon - \bar{e}_j}\right)(\epsilon S - F^f)_{\sigma\tau} \mathrm{P}\int_{-\infty}^{+\infty} dt\, \frac{\rho^f_{\tau\nu}(t)}{\epsilon - t}\right]$$
$$-\pi i \sum_j \left[\delta(\epsilon - \bar{e}_j)\bar{a}_{\mu j}\bar{a}_{\sigma j} \mathrm{P}\int_{-\infty}^{+\infty} dt\,(\epsilon S - F^f)_{\sigma\tau}\,\frac{\rho^f_{\tau\nu}(t)}{\epsilon - t} + \mathcal{P}\left(\frac{\bar{a}_{\mu j}\bar{a}_{\sigma j}}{\epsilon - \bar{e}_j}\right)(\epsilon S - F^f)_{\sigma\tau}\rho^f_{\tau\nu}(\epsilon)\right], \tag{8}$$

we obtain, after performing the integration indicated in the last line of Eq. (5),

$$P^{AA,AB,BA}_{\mu\nu} = 2\sum_j \bar{a}_{\mu j}\bar{a}_{\nu j}\Theta(\epsilon^f_F - \bar{e}_j)\,,$$
$$P^{BB}_{\mu\nu} = 2\sum_j \sum_\sigma^B \bar{a}_{\mu j}\bar{a}_{\sigma j} m_{\sigma\nu}(\bar{e}_j) \tag{9}$$

where

$$m_{\sigma\nu}(e) = \sum_\tau^B \mathrm{P}\int_{-\infty}^{+\infty} dt\,\frac{(eS - F^f)_{\sigma\tau}\rho^f_{\tau\nu}(t)}{e - t}\,\Theta(\epsilon^f_F - e)$$
$$+ \sum_\tau^B \mathrm{P}\int_{-\infty}^{\epsilon^f_F} dt\,\frac{(tS - F^f)_{\sigma\tau}\rho^f_{\tau\nu}(t)}{t - e}\,. \tag{10}$$

In (8) and (10) $\mathcal{P}$ indicates "principal part of" and P in front of the integral sign denotes the Cauchy principal value: $\rho^f(t)$ is the projected density of states for the free system at energy $t$,

$$\rho^f_{\tau\nu}(t) = \frac{d}{dt}(a^f_{\tau i}a^f_{\nu i})\,.$$

If a finite basis set is used in each crystal cell, $\rho$ is different from zero only in a finite energy interval, that is from $E_m$, bottom of the lowest band, to $E_M$, top of the highest conduction band.

The matrix element $m_{\sigma\nu}(e)$ can be written in a more handy form. For $e < \epsilon^f_F$ we have

$$m_{\sigma\nu}(e) = \sum_\tau^B \left[\int_{E_m}^{\epsilon^f_F} dt\, S_{\sigma\tau}\rho^f_{\tau\nu}(t) + \int_{\epsilon^f_F}^{E_M} dt\,\frac{(eS_{\sigma\tau} - F^f_{\sigma\tau})\rho^f_{\tau\nu}(t)}{e - t}\right]$$
$$= \sum_\tau^B \left[\int_{E_m}^{E_M} dt\, S_{\sigma\tau}\rho^f_{\tau\nu}(t) + \int_{\epsilon^f_F}^{E_M} dt\,\frac{(tS_{\sigma\tau} - F^f_{\sigma\tau})\rho^f_{\tau\nu}(t)}{e - t}\right] \tag{11}$$

and a similar expression is obtained for $e > \epsilon^f_F$. Introducing the quantities

$$d_{\sigma\nu} = \int_{E_m}^{E_M} dt \sum_\tau^B S_{\sigma\tau}\rho^f_{\tau\nu}(t)\,,$$
$$\alpha_{\sigma\nu}(t) = \sum_\tau^B (tS_{\sigma\tau} - F^f_{\sigma\tau})\rho^f_{\tau\nu}(t)\,, \tag{12}$$

we finally have

$$m_{\sigma\nu}(e) = d_{\sigma\nu} - \int_{\epsilon^f_F}^{E_M} dt\,\frac{\alpha_{\sigma\nu}(t)}{(t - e)}\,; \quad e < \epsilon^f_F\,,$$
$$m_{\sigma\nu}(e) = \int_{E_m}^{\epsilon^f_F} dt\,\frac{\alpha_{\sigma\nu}(t)}{(t - e)}\,; \quad e > \epsilon^f_F\,. \tag{13}$$

Formulas (12) and (13) are very practical for the computation of $m_{\sigma\nu}(e)$ since no poles are left in the integration interval and all summations over $\tau$ may be effected preliminarily when calculating the function $\alpha_{\sigma\nu}(t)$ and the constant $d_{\sigma\nu}$. Note that, in any orthogonal basis, $d_{\sigma\nu} = \delta_{\sigma\nu}$.

We have so arrived at the definition of a nonsymmetric adimensional energy-dependent coupling matrix $M(e)$ [with elements $m_{\sigma\nu}(e)$], which, through Eq. (9), insures the connection of the cluster with the defective solid. The size of each $M$ matrix is $n_B \times n_B$, where $n_B$ is the number of basis functions belonging to set $B$.

A fundamental characteristic of $M$ is that it only depends on the electronic structure of the free solid (through $F^f, \rho^f, \epsilon^f_F$); so it is the same for any adsorbate in any geometrical arrangement and can be said to summarize the adsorptive properties of the surface. $F^f$, $\rho^f$, and $\epsilon^f_F$ are evidently independent of the particular cluster (and so is $d_{\sigma\nu}$ in an orthogonal basis) but $M$ depends on the cluster size because $\alpha_{\sigma\nu}(t)$ is a cluster dependent quantity through the summation $\sum^B_\tau$.

Note finally that the dependence of $M$ on energy is connected to the distribution of the virtual states of the free solid for $e<\epsilon_F^f$ and to the distribution of the occupied states for energies above the Fermi level. It may be so qualitatively stated that the $M$ matrix introduces hole-electron interactions between the cluster and the defective solid.

### B. Limiting conditions

We now show that the equations obtained are correct in the limiting conditions. When the interaction with $A$ is negligible (for definiteness, take $A$ to be absent), we have, for a cluster of arbitrary size,

$$F^C = F^f,$$
$$\sum_{\sigma}^{B} \bar{a}_{\sigma j} F^f_{\sigma\tau} = \sum_{\sigma}^{B} \bar{e}_j \bar{a}_{\sigma j} S_{\sigma\tau}, \tag{14}$$
$$\sum_{\sigma}^{B} \bar{a}_{\sigma j} \alpha_{\sigma\nu}(t) = \sum_{\sigma\tau}^{B} \bar{a}_{\sigma j}(t-\bar{e}_j) S_{\sigma\tau} \rho^f_{\tau\nu}(t).$$

Substitution in Eq. (9), and (11)–(12) gives, keeping into account that $\overline{AA}^{\dagger} S = I$,

$$P^C_{\mu\nu} = 2\sum_{\sigma}^{B}\Bigg[\sum_{j(\bar{e}_j<\epsilon_F^f)} \bar{a}_{\mu j}\bar{a}_{\sigma j}\Big(d_{\sigma\nu} - \sum_{\tau}^{B}\int_{\epsilon_F^f}^{E_M} dt\, S_{\sigma\tau}\rho^f_{\tau\nu}\Big) + \sum_{j(\bar{e}_j>\epsilon_F^f)} \bar{a}_{\mu j}\bar{a}_{\sigma j}\sum_{\tau}^{B}\int_{E_m}^{\epsilon_F^f} dt\, S_{\sigma\tau}\rho^f_{\tau\nu}\Bigg]$$
$$= 2\sum_{\tau}^{B}\Bigg[\sum_{j}\Big(\sum_{\sigma}^{B}\bar{a}_{\sigma j}S_{\sigma\tau}\Big)\bar{a}_{\mu j}\Bigg]\int_{E_m}^{\epsilon_F^f} dt\,\rho^f_{\tau\nu}$$
$$= \rho^f_{\mu\nu}. \tag{15}$$

We find, therefore, as we should, that at self-consistency, the solution obtained by using the embedding procedure coincides with the solution for the infinite solid. For instance, if the $B$ set is reduced to the valence orbitals on a single atom, $F$ is diagonal and $S$ is unity so that $\bar{A}$ is also unity, it is then obvious that $M$ is diagonal and that it should assume, at $e=F^f_{\nu\nu}$, the value $P^f_{\mu\mu}/2$. In the other extreme case, when $B$ is very large, we have, for $\sigma$ near $A$,

$$\sum_{\tau}^{B} F^f_{\sigma\tau}\rho^f_{\tau\nu}(t) \simeq \sum_{\tau}^{S} F^f_{\sigma\tau}\rho^f_{\tau\nu}(t) \tag{16}$$
$$= \sum_{\tau}^{S} tS_{\sigma\tau}\rho^f_{\tau\nu}(t),\quad d_{\sigma\nu}\simeq\delta_{\sigma\nu},$$

whence

$$\alpha(t)\simeq 0,\quad m_{\sigma\nu}(e)\simeq\delta_{\sigma\nu}\Theta(\epsilon_F^f - e), \tag{17}$$

as expected.

### C. Method of calculation

Having derived the basic equations (7), (9), (12), (13) a scheme of calculation can be proposed. First, the free solid quantities $F^f$, $S^f$, $\rho^f$ must be obtained within $B$. If $\vec{g}'$, $\vec{g}''$ are general vectors of the bidimensional translational group parallel to the surface, we can write

$$F^f_{\sigma\nu} \equiv F^f_{\bar{\sigma}\vec{g}',\bar{\nu}\vec{g}''} = F^f_{\bar{\sigma}0,\bar{\nu}(\vec{g}''-\vec{g}')}. \tag{18}$$

Here $\bar{\sigma}$ and $\bar{\nu}$ correspond to a numeration of the basis functions within each cell, whereas $\sigma$, $\nu$ refer to a numeration within the whole cluster $B$. Similar expressions hold true for $S^f$ and $\rho^f$.

Usually, the solution for the free solid is known at a discrete number of appropriately chosen[25,26] $\vec{k}_j$ points in the irreducible part of the bidimensional Brillouin zone. The quantities $F_{\sigma\nu}$ and $S_{\sigma\nu}$ may be obtained by a weighted sum over these points, after application of all point group symmetry operators $\hat{R}$,[27] the weights $W_j$ depending on the choice of the sampling points,

$$F^f_{\bar{\sigma}0,\bar{\nu}\vec{g}} = \sum_j W_j\Big[\frac{1}{h}\sum_{\hat{R}} F_{\bar{\sigma}\bar{\nu}}(\vec{k}_j^R)e^{-i\vec{k}_j^R\cdot\vec{g}}\Big]. \tag{19}$$

Here $h$ is the order of the point group.

More attention must be paid when calculating the projected densities of states $\rho^f_{\tau\nu}(t)$, since they involve integration over a limited portion of the Brillouin zone. The method due to Monkhorst[26] seems best suited to this purpose, and is applied here to perform integrals of the form $I(\epsilon) = \int_{BZ} dk\, f(k)\Theta(\epsilon-\omega(k))$, $\omega$ and $f$ being totally symmetric functions of $\vec{k}$. Conceptually, it requires reconstructing $f$ and $\omega$ at a closely spaced net in $k$ space, using a truncated Fourier expansion. In each small domain defined by the close net, linear interpolation of $f$ and $\omega$ is used[28] and the integral is analytically performed. In practice, it is easily shown that this procedure is equivalent to

$$I(\epsilon)\simeq\sum_j f(\vec{k}_j)\alpha_j(\epsilon), \tag{20}$$

where the weights $\alpha_j$ depend on the level $\epsilon$, on the $k$ dependence of $\omega$, and, to a certain extent, on the closeness of the reconstructed net, but are totally independent of $f(\vec{k})$.

In the present case, weights $\alpha^i_j(\epsilon_m)$ may be calculated for each energy band $\omega^f_i(\vec{k})$ at a certain number of closely spaced energy points $\epsilon_n$, and we have

$$\rho^f_{\bar{\sigma}0,\bar{\nu}\vec{g}}(t_n) \simeq \frac{1}{\Delta\epsilon}\sum_{ij}[\alpha^i_j(\epsilon_{n+1}) - \alpha^i_j(\epsilon_n)] \times \frac{1}{h}\sum_{\hat{R}} a^*_{\bar{\tau}i}f(\vec{k}_j^R)a^f_{\bar{\nu}i}(\vec{k}_j^R)e^{-i\vec{k}_j^R\cdot\vec{g}}, \tag{21}$$
$$t_n = \tfrac{1}{2}(\epsilon_n+\epsilon_{n+1}).$$

Using (19) and (21), $F, S, \rho$ can be calculated once and for all for an appropriate number of combinations $\bar{\sigma}0, \bar{\nu}\vec{g}$ covering all non-negligible terms.

Second, the actual $B$ cluster is chosen. The $M$ matrix is calculated according to Eq. (11) and (12) at energy points $e_i$ sufficiently closely spaced for a linear interpolation procedure to be adequate. In principle, we do not know the interval of energy that must be spanned by the sampled points to contain all possible $\bar{e}_j$ values that will be encountered. In practice the behavior of $M$ is very smooth outside the interval $(E_m - E_M)$, and few energy points widely spaced outside this interval are sufficient. On the contrary, very close spacing should be chosen near the Fermi level; not only $M$ elements are discontinuous there, but their variations are more rapid in its vicinity. The $M$ matrices should be stored in order of increasing energy for further use.

The cluster calculation can now be performed. The correction matrix $L^B$ must first be calculated [see Eq. (6)]. It is easily seen that in the CNDO approximation and for an homonuclear solid $L^B$ is zero.

In the SCF step, a subroutine must be supplied for the iterative recalculation of the $P$ matrix according to Eq. (9); instead of $m_{\sigma\nu}(\bar{e}_j)$ we can use a weighted mean of $m_{\sigma\nu}(e_i)$, $m_{\sigma\nu}(e_{i+1})$, $e_i$, and $e_{i+1}$ being the energy-sampled points immediately below and above $\bar{e}_j$. The time taken by the triple matrix multiplication in (9) is of the same order of magnitude of the diagonalization (7), since about $n^4$ operations and required in both cases. In future work, advantage could be taken of the quasidiagonal structure of $M$ near the center of the cluster (see below), to reduce the number of operations.

Finally, differential quantities can be obtained from the solution, by admitting, according to approximation (a), that the $P$ matrix and the $F$ matrix are unchanged except within the cluster. In particular, for the chemisorption energy we have, in the Hartree-Fock approximation,

$$\Delta E = \tfrac{1}{2}\,\mathrm{Tr}^C P(F+H) - \tfrac{1}{2}\,\mathrm{Tr}^B P^f(F^f+H^f) - E_A + \Delta E_n . \tag{22}$$

Here $\mathrm{Tr}^C$ and $\mathrm{Tr}^B$ mean that matrix multiplications and summations are performed within $C$ and $B$, respectively, $E^A$ is the formation energy of the species $A$ from its nuclei and electrons calculated in the same approximation as the rest, and $\Delta E_n$ is the electrostatic interaction between the system of nuclei in $A$ with those in $B$.

In this formula, it is assumed that the cluster is neutral; if a charge $\Delta q$ is left on the cluster, a correction term $\mu\Delta q$ should be added where $\mu$ is the chemical potential of electrons in the free solid.

## III. RESULTS AND DISCUSSION

As anticipated, chemisorption of a hydrogen atom on a graphite monolayer was chosen for a preliminary test of the method, using the NDO approximation in the CNDO-2 version of Pople and Beveridge.[29] Only closed shell configurations were studied. On-atom adsorption was considered, so a reasonable though not mandatory choice of the $B$ cluster comprises a certain number of shells of neighbors of the reference 0 atom on which adsorption takes place (see Fig. 2).

The CNDO approximation uses Slater-type valence orbitals as basis functions, but treats them as orthogonalized Löwdin orbitals,[30] so the $S$ matrix is unity. The $F^f$ matrix elements for graphite were calculated from the solution previously obtained[11] according to Eq. (19), for all the relative positions $(\bar{\sigma}0, \bar{\nu}\vec{g})$ occurring in the 13-atoms cluster labelled as IV in Fig. 2; all other $F^f$ elements are negligible in practice. For calculating the projected densities of states $\rho^f_{\sigma 0, \bar{\nu}\vec{g}}$ at the same relative positions, the procedure discussed in Sec. II C was used. The energy bands $\omega^f_i(\vec{k})$ were reconstructed following the Monkhorst scheme at the intersection point of a commensurate net in the reciprocal space, comprising 2304 points in the Brillouin zone. In each triangular domain of this net, linear interpolation was used. It was then possible to calculate the weights $\alpha^i_j(\epsilon_n)$ at 51 energy points $\epsilon_n$ uniformly spaced from the bottom of the lowest band (−2.12 a.u.) to the top of the highest conduction band (+0.60 a.u.) for each $i$ band and for the

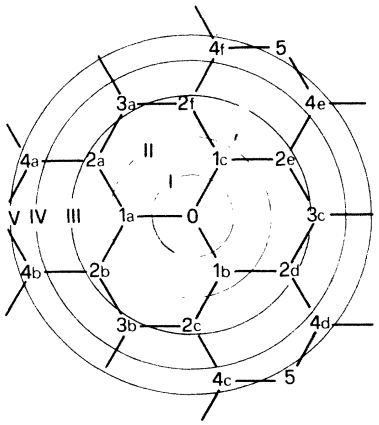


FIG. 2. Numeration of the carbon atoms of graphite and identification of progressively larger $B$ clusters: I (1 atom); II (4 atoms); III (9 atoms); IV (13 atoms); V (19 atoms). The hydrogen adsorption takes place at the central (0) atom.

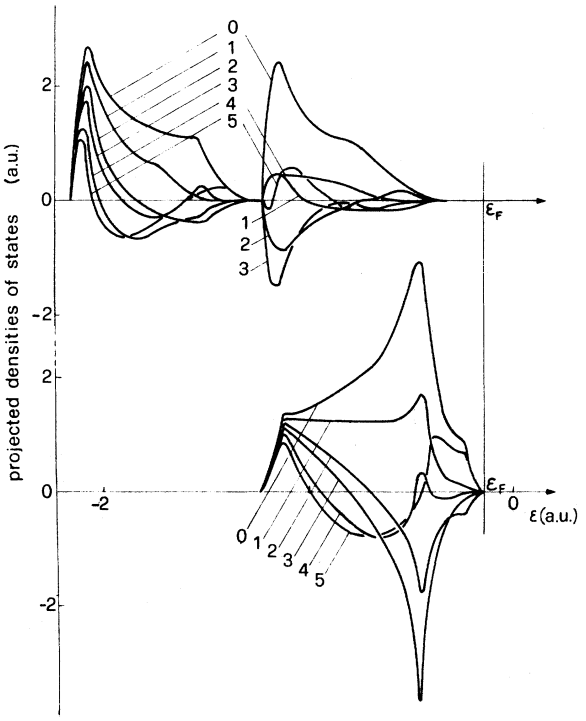


FIG. 3. Projected densities of states $\rho^f_{s\,0,\,sm}(\epsilon)$ (top figure) and $\rho^f_{z\,0,zm}(\epsilon)$ (bottom figure). The index $m$, which labels the different curves corresponds to the numeration of atoms in Fig. 2; $z$ indicates the orbital $p_z$, orthogonal to the graphite layer. Densities of states above the Fermi level are not drawn.

19 $\vec{k}_j$ points included in the irreducible part of the first Brillouin zone where an explicit self-consistent solution for graphite was available. The projected densities of states were finally obtained at the 50 intermediate $t_n$ points according to Eq. (21).

In Fig. 3, some $\rho^f$ elements are reproduced as a function of energy; only energies below $\epsilon^f_F$ (−0.13 a.u.) are considered, since the oscillations above $\epsilon^f_F$ are so rapid as to make the graph unreadable there. It is seen that the decrease of $\rho^f_{\mu\nu}$, (hence, $\mathrm{Im}G_{\mu\nu}$) with increasing distance between $\mu$ and $\nu$ centers is not very rapid. However, due to the oscillatory character of $Q_{\mu\nu}(\epsilon)$ and $\rho^f_{\mu\nu}(\epsilon)$ at given energies for different relative positions, large cancellations of terms do in fact take place when effecting the sums $\sum^B$ or $\sum^D$, so making it more justifiable to accept approximation $b$ of Sec. II.

Having chosen the actual $B$ cluster, the $M(e)$ matrices were calculated according to formulas (12) and (13) at 72 energy points within the interval $E_m - E_M$ not uniformly spaced but more densely concentrated near $\epsilon^f_F$. Two additional matrices

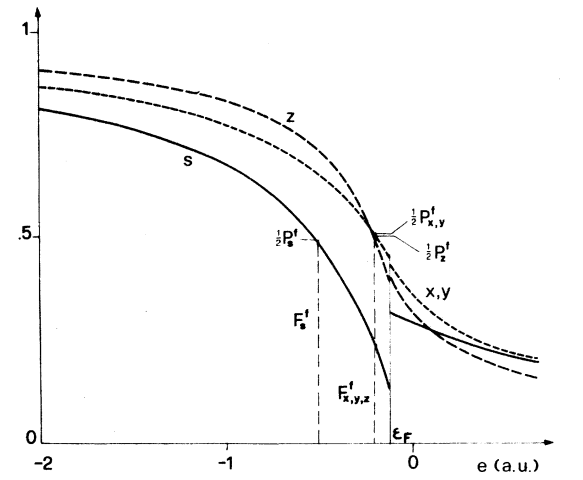


FIG. 4. Diagonal elements of $M^I$ as a function of energy; nondiagonal elements are zero. $F^f_S$ is an abridged notation for $F^f_{SS}$, and analogously for the other symbols.

were calculated at − 10 a.u. and +10 a.u. in order to encompass all possible values for $\bar{e}_j$. This choice was adequate to justify linear interpolation of $M$ matrices between adjacent energy values. Figures 4–6 are introduced to give an idea of the structure of the coupling matrices, of their dependence on energy and on their variation with the choice of the cluster $B$.

Figure 4 represents the extreme case of the diagonal $M^I$ matrix, corresponding to a one-atom cluster: each basis function is here at the same time a "central" and a "border" function; it is shown that $M^I_{\mu\mu}(F^f_{\mu\mu})$ equals one half the electron population in infinite graphite, as discussed in Sec. II B.

In Fig. 5, referring to the four-atom cluster,

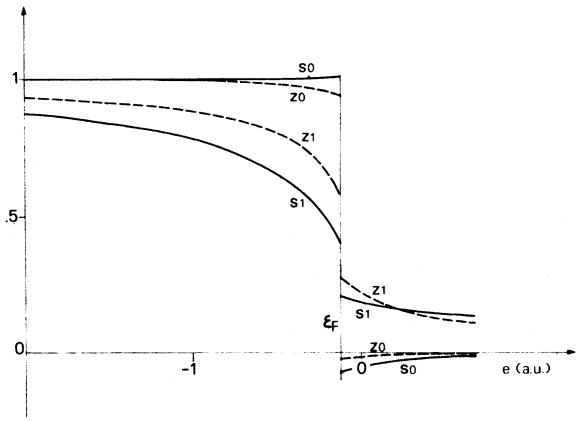


FIG. 5. Diagonal $sm$ amd $zm$ elements of $M^{II}$, $m$ labeling the two different types of atoms, 0 and 1, in the cluster (see Fig. 2).

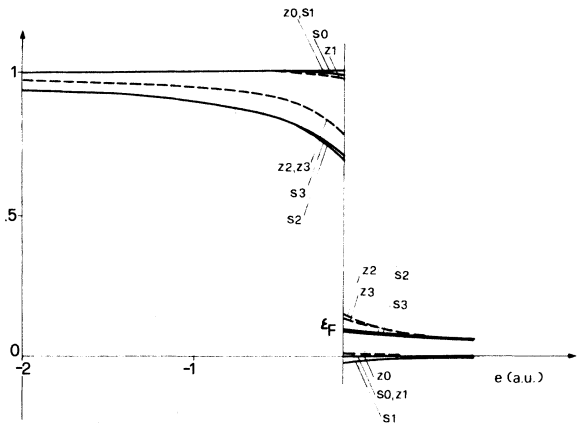


FIG. 6. Diagonal $sm$ and $zm$ elements of $M^{IV}$ (see Fig. 2).

it is seen that the diagonal elements on the central atom already approach quite closely the asymptotic $\Theta(\epsilon_F^f - e)$ behavior [see Eq. (17)]. Note that also diagonal elements on border atoms have a $\Theta$-like behavior, more clearly so at least than in $M^I$, each border atom being here directly connected to the internal atom.

These trends are further enhanced in $M^{IV}$, as shown in Fig. 6. The $\Theta$-function behavior is approximately perfect for the four internal atoms, especially for the central one; in this sense also border atoms seem here to be more "internal" than border atoms in the cluster II. In fact, each border atom is here directly connected to two other atoms in the cluster, whereas, in II, the atoms of type 1 had only one nearest neighbor belonging to the cluster.

Out of diagonal elements of the $M$ matrices are generally much smaller than diagonal ones and become progressively less important as the distance between the centers of the related functions is increased. Both these characteristics are more pronounced for $s$-type than for $\pi$-type functions. Their dependence on energy, except for the discontinuity at the Fermi level, is quite smooth.

As a general comment, it may be observed that the coupling matrices exhibit a dependence on energy which is much smoother than expected from the complicated behavior of the $\rho$ functions from which they derive; and also the asymptotic $\Theta$-function behavior is found to be obeyed, in first approximation, by all but the border functions. These findings are encouraging and could suggest the use of more efficient interpolation techniques than the linear one, with saving of computer time and storage.

A test of the numerical accuracy of the calculated $M$ matrices and of the correctness of the method was performed by applying the embedding procedure, Eqs. (7) and (9), to a cluster of graphite atoms in the absence of any adsorbate, and comparing the results with those obtained for infinite graphite and for the nonembedded cluster. Table I shows the outcome of such a calculation for cluster IV, similar results having been obtained for all clusters I–V. It is seen that atomic-orbital populations reproduce those obtained for infinite graphite to within one-thousandth of an electron, and a comparable accuracy is found for extradiagonal elements of $P$. On the other hand, the electronic state of the nonembedded cluster is very different from that of graphite even in neighborhood of the central atom, so making it questionable, from the start, whether the adsorption characteristics of clusters of that size adequately reproduce those of the infinite solid.

The adsorption of hydrogen above a carbon atom of graphite was studied in particular for the embedded clusters II and IV; the results obtained are displayed in Figs. 7–9.

In performing these calculations, difficulties were encountered in the attainment of convergency, of the type often reported in literature.[11,31,32]

TABLE I. Comparison of $P_{\mu\nu}$ matrix elements for graphite, embedded cluster (IV) and nonembedded cluster (IV) in the absence of adsorbates. Symbols for identifying the basis functions $\mu$, $\nu$ are chosen with reference to Fig. 2. For instance, $x2a$ denotes the $p_x$ atomic orbital on atom $2a$.

| $\mu$, $\nu$ | Graphite | Embedded cluster | Nonembedded cluster |
|---|---|---|---|
| $s0$, $s0$ | 0.9806 | 0.9807 | 1.0107 |
| $s1$, $s1$ | 0.9806 | 0.9807 | 0.9680 |
| $s2$, $s2$ | 0.9806 | 0.9807 | 1.2309 |
| $s3$, $s3$ | 0.9806 | 0.9809 | 1.1081 |
| $z0$, $z0$ | 1.0010 | 1.0004 | 0.9546 |
| $z1$, $z1$ | 1.0010 | 1.0005 | 1.1291 |
| $z2$, $z2$ | 1.0010 | 1.0006 | 0.7086 |
| $z3$, $z3$ | 1.0010 | 1.0008 | 1.1341 |
| $x0$, $x0$ | 1.0092 | 1.0097 | 1.0524 |
| $x1a$, $x1a$ | 1.0092 | 1.0097 | 0.9264 |
| $x2a$, $x2a$ | 1.0092 | 1.0100 | 1.1988 |
| $x3a$, $x3a$ | 1.0092 | 1.0100 | 0.6805 |
| $s0$, $s1$ | 0.312 | 0.311 | 0.331 |
| $s0$, $s2$ | 0.004 | 0.004 | 0.013 |
| $s0$, $s3$ | −0.040 | −0.040 | −0.002 |
| $z0$, $z1$ | 0.524 | 0.524 | 0.527 |
| $z0$, $z2$ | −0.000 | −0.000 | 0.012 |
| $z0$, $z3$ | −0.184 | −0.183 | −0.234 |
| $s0$, $x1a$ | 0.478 | 0.478 | 0.458 |
| $s0$, $x2a$ | −0.238 | −0.239 | −0.229 |
| $s0$, $x3a$ | −0.016 | −0.015 | −0.052 |

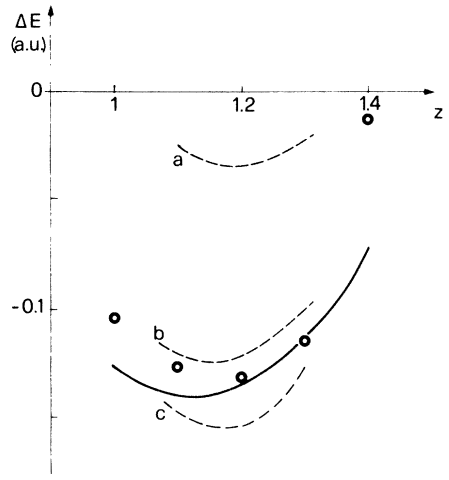


FIG. 7. Chemisorption energy $\Delta E$ as a function of hydrogen distance from the surface. The full curve is a best fit to results obtained for the 13-atom embedded cluster, the circles refer to results for the four-atom embedded cluster. Dashed curves a, b, c give the chemisorption energy per atom in regular on-atom chemisorption for 1:2 (Ref. 11), 1:1 (Ref. 33) and 1:18 (Ref. 31) hydrogen-to-carbon ratios.

The problem was more serious with large clusters, due to the increase in degrees of freedom; it is also possible that imposing boundary conditions corresponding to the connectivity with an infinite solution makes, in general, the convergence problem more critical than with a finite cluster. The classical expedients were used here of using as trial starting solution that one found at a nearby configuration where convergency has been attained, and of mixing $P$ matrices from different iterations during the self-consistency step. Still, some difficulties were left deserving further critical work, especially concerning the chemisorption energy $\Delta E$, which is the near-zero difference between two very large quantities [see Eq. (22)].

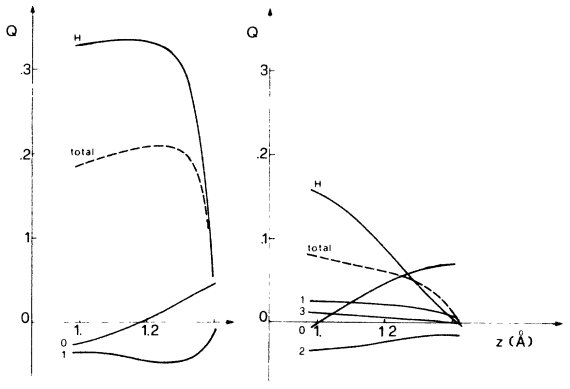


FIG. 8. Net charge on atoms as a function of hydrogen distance from the surface calculated for the four-atom (left-hand side) and the 13-atom (right-hand side) embedded clusters. The numbers (0,1,2,3) which label the curves correspond to the numeration of graphite carbon atoms in Fig. 2. The dashed curve is the total net residual charge in the cluster.

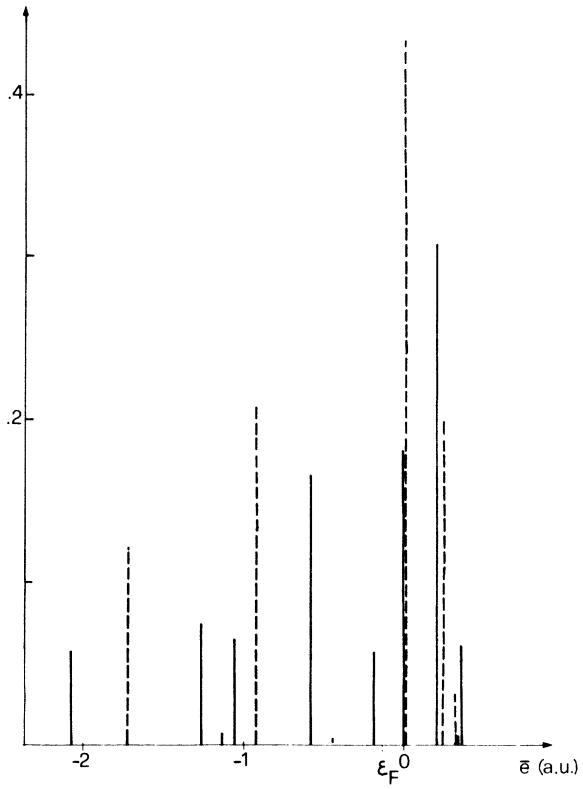


FIG. 9. Spectrum of hydrogen contributions to the density of states: for each eigenvector the quantity $|\bar{a}_{Hj}|^2$ is reported at energy $\bar{\varepsilon}_j$. Full lines refer to chemisorption on the 13-atom embedded cluster for a hydrogen distance of 1.1 Å from the surface, dashed lines refer to the same case for the four-atom cluster.

In Fig. 7 the chemisorption energy is given as a function of distance of $H$ from the surface, calculated according to (22) with correction for non-neutrality included. The full curve is the result of a best-fit procedure performed on 17 solutions obtained for cluster IV after eight iteration cycles in the interval 1.0–1.4 Å, starting from different trial $P$ matrices; the related standard deviation is 0.01 a.u. The results obtained for the four-atom cluster fit rather nicely, perhaps fortuitously, with this curve. In any case the equilibrium configuration is identified at about 1.15 Å from the surface, which is the same value obtained in the case of regular on-atom chemisorption. Comparison with the results obtained in that case

seems to indicate that the chemisorption energy for the isolated atom is nearer to the values obtained in the 1:1 (Ref. 33) than in the 1:2 (Ref. 11) concentrations and approaches the value obtained by Bennett *et al.*[31] in the 1:18 concentration using the periodic boundary condition method and the same CNDO-2 parametrization. Even if possibly subject to revision because of the uncertainties just mentioned, this result is interesting, since it seems to confirm the fact that chemisorption energy is a quantity strongly dependent on structure and that extrapolation of results from more to less dense phases or vice versa is hazardous.[22]

While from the point of view of the chemisorption energy the four-atom embedded cluster seems to give unexpectedly good results, the need for a sufficiently large $B$ cluster where to allow for self-consistency becomes apparent when looking at quantities more specifically related to the electronic state of the system, such as the net atomic charge on the atoms calculated according to a classical Mulliken analysis. In Fig. 8 the net charges on the different types of atoms are reported as a function of the distance of H from the surface, together with the total charge in the cluster.

Some qualitative features of these results are similar for the two clusters. A group of positively charged atoms is found at the center of the cluster, the positive charge being particularly high on hydrogen, surrounded by a ring of negative atoms. Beyond these two regions, an external ring of positive charges of small entity is observed in the larger cluster so suggesting the occurrence of quenched Friedel oscillations; a test effected on the 19-atom cluster (labeled V in Fig. 2) for a H distance of 1.2 Å has given negligible, but still positive, charge on the six atoms of type 4. An alternancy of positive charges on the hydrogen atom and the underlying carbon atom and of negative charge on the other carbon atoms was also observed in regular 1:2 chemisorption.[22] A progressive decrease of the positive charge on the H atom and a parallel increase of the charge on the underlying carbon atom with increasing distance is also found in both cases.

Apart from these qualitative similarities, quantitative results are very different for the two clusters. In particular, we must consider the net residual charge in the cluster, which is found as a consequence of fixing the Fermi level at its free-solid value. In the small cluster the residual charge is at least three times as large as in the bigger one; at the equilibrium distance, in the latter case, a net charge of only 0.06 electrons is observed, which is a very satisfactory result, if one considers that a total of 53 valence electrons are assigned to the cluster; furthermore, it is still an open question whether this residual charge is essentially to be attributed to an insufficient size of the cluster or to numerical inaccuracies. In any event, for cluster IV, the $P$-matrix elements at the border are already close to their free-graphite values.

The structure of eigenvalues and eigenvectors can contribute to the description of the electronic state for the different solutions. In Fig. 9 the spectrum of the hydrogen contributions to the different eigenvectors is provided for a distance of 1.1 Å, in the two cases. As expected by elementary symmetry considerations, only few eigenvectors have an appreciable contribution from the hydrogen atom: 6 out of 17 and 10 out of 53 for the two clusters respectively; all of them are found to correspond not to localized states but to resonant ones, asymptotically merging into free-solid solutions. A comparison of the two spectra suggests that the smaller cluster has still too poor a basis to adequately simulate the density of states on hydrogen; this may be the main reason why the charge on hydrogen is so different in the two cases. Another characteristic of the spectrum which is worth mention is the concentration of important peaks near the Fermi level. This fact had been observed in previous studies of on-atom adsorption of hydrogen on graphite[11,34] and may be in part responsible for the problems of convergency that were encountered.

In summary, these preliminary tests seem to indicate that the embedding scheme here proposed is workable in practice, although further work is surely needed to speed up the computing procedures and to devise more efficient numerical techniques for reaching and testing convergency. The approximations which are at the basis of the method appear to be adequate for moderately large clusters, such as the 13-atom one, labeled here as IV; for smaller clusters, such as the II one, the approximation corresponding to admit that the influence of the adsorbate on the electronic state does not extend beyond the $B$ region is surely incorrect. It was not possible to effect, for the system here considered, a comparison with chemisorption on the nonembedded cluster in the same approximation, since an odd number of electrons would be involved in that case so preventing any closed-shell solution. This fact in itself is an argument in favor of the superiority of the embedding scheme with respect to an isolated cluster approach; in any case, the electronic state of the isolated cluster with no adsorbate was so different from the state of infinite graphite for the sizes here explored, that the boundary effects would be

surely important in characterizing chemisorption.

Concerning further developments of the method apart from obvious extensions to other systems and geometries, it would be possible to extend it to study strictly local geometrical rearrangements of the adsorbent atoms induced by adsorption. Finally, a formally identical scheme could be used to connect a surface solution to the solution for a tridimensional solid,[35,36] so reducing the self-consistency problem to few layers, within a crystalline orbital SCF formalism.

ACKNOWLEDGMENTS

The author is grateful to Dr. C. Moser for an invitation to a CECAM workshop on "Structure of Surfaces and Small Molecules Adsorbed on Surfaces", held in Orsay, where a large part of the work for developing and testing the computer programs was performed; the workshop offered the opportunity for stimulating discussions with participants, especially with B. Lévy and B. McMaster. The author would also like to thank Professor T.B. Grimley for helpful comments and discussions.

[1]D. W. Ellis, E. J. Baerends, H. Adachi, and F. W. Arrill, Surf. Sci. 64, 649 (1977).
[2]C. W. Bauschlicher Jr., D. H. Liskow, C. F. Bender, and H. F. Schaefer III, J. Chem. Phys. 62, 4815 (1975).
[3]H. Stoll and H. Preuss, Surf. Sci. 65, 229 (1977).
[4]C.H. Li and J. W. D. Connolly, Surf. Sci. 65, 700 (1977).
[5]G. Blyholder, J. Chem. Phys. 62, 3193 (1975).
[6]A. B. Anderson and R. H. Hoffmann, J. Chem. Phys. 61, 4545 (1974).
[7]T. B. Grimley and E. E. Mola, J. Phys. C 9, 3437 (1976).
[8]J. A. Appelbaum and D. R. Hamann, Phys. Rev. Lett. 34, 806 (1975); 36, 450 (1976); Phys. Rev. B 6, 2166 (1972).
[9]S. G. Louie, K. M. Mo, J. R. Chelikowsky, and M. L. Cohen, Phys. Rev. B 15, 5627 (1977).
[10]K. M. Ho and M. L. Cohen, Phys. Rev. B 15, 3888 (1977).
[11]R. Dovesi, C. Pisani, F. Ricca and C. Roetti, J. Chem. Phys. 65, 3075 (1976).
[12]T. B. Grimley, in *Proceedings of the International School of Physics Enrico Fermi, Course LVIII,* edited by F. D. Goodman (Compositori, Bologna, 1974), p. 298.
[13]T. B. Grimley, in *Electronic Structure and Reactivity of Metal Surfaces*, edited by E. G. Derouane and A. A. Lucas (Plenum, New York, 1976), p. 113.
[14]T. B. Grimley and C. Pisani, J. Phys. C 7, 2831 (1974).
[15]O. Gunnarsson and H. Hjelmberg, Phys. Scr. 11, 97 (1975).
[16]O. Gunnarsson, H. Hjelmberg, and B. I. Lundqvist, Surf. Sci. 63, 348 (1977).
[17]W. Kohn and L. J. Sham. Phys. Rev. 140, A1133 (1965).
[18]G. Doyen, Surf. Sci. 59, 461 (1976).
[19]G. Doyen and G. Ertl, Surf. Sci. 65, 641 (1977).
[20]A. V. Bandura and R. A. Evarestov, Phys. Status Solidi B 64, 635 (1974).
[21]R. C. Baetzold, J. Phys. Chem. 80, 1504 (1976).
[22]R. Dovesi, C. Pisani, F. Ricca, and C. Roetti, Surf. Sci. (to be published).
[23]A. Yaniv and W. Kohn (unpublished).
[24]A. Many, Y. Goldstein, and N. B. Grover, in *Semiconductor Surfaces* (North-Holland, Amsterdam, 1965).
[25]D. J. Chadi and M. L. Cohen, Phys. Rev. B 8, 5747 (1973).
[26]H. J. Monkhorst and J. D. Pack, Phys. Rev. B 13, 5188 (1976).
[27]R. Dovesi, C. Pisani, F. Ricca, and C. Roetti, Chem. Phys. Lett. 39, 103 (1976).
[28]G. Gilat and L. J. Raubenheimer, Phys. Rev. 144, 290 (1966).
[29]J. A. Pople and D. L. Beveridge, *Approximate Molecular Orbital Theory* (McGraw-Hill, New York, 1970).
[30]P. O. Löwdin, J. Chem. Phys. 18, 365 (1950).
[31]A. J. Bennett, B. McCarroll, and R. P. Messmer, Phys. Rev. B 3, 1397 (1971).
[32]M. R. Hayns, Theor. Chim. Acta 39, 61 (1975).
[33]R. Dovesi, C. Pisani, F. Ricca, and C. Roetti, J. Chem. Phys. 65, 4116 (1976).
[34]N. V. Cohan, M. B. Gordon, and M. Weissman, Solid State Commun. 22, 181 (1977).
[35]A. Van der Avoird, S. P. Liebmann, and D. J. M. Fassaert, Phys. Rev. B 10, 1230 (1974).
[36]S. P. Liebmann, A. Van der Avoird, and D. J. M. Fassaert, Phys. Rev. B 11, 1583 (1974).